pp. 1–16 (2012)

Modelling of thrombus growth and growth stop in flow by the method of dissipative particle dynamics

A. TOSENBERGER*[2], F. ATAULLAKHANOV[3456], N. BESSONOV[7], M. PANTELEEV[3456], A. TOKAREV[34], and V. VOLPERT *[28]

Abstract — Platelet aggregation at the site of the vascular injury leads to the formation of a hemostatic plug covering the injury site, or a thrombus in the pathological case. The mechanisms that control clot growth or lead to growth arrest are not yet completely understood. In order to study these mechanisms theoretically, we use the Dissipative Particle Dynamics method, which allows us to model individual platelets in the flow and in the clot. The model takes into account different stages of the platelet adhesion process. First, a platelet is captured reversibly by the aggregate, then it is activated and adheres firmly, becoming a part of its core. We suggest that the core of the clot is composed of platelets unable to attach new platelets from the flow due to their activation by thrombin and/or wrapping by the fibrin mesh. The simulations are in a good agreement with the experimental results [9]. Modelling shows that stopping the growth of a hemostatic plug (and thrombus) may result from its exterior part being removed by the flow and exposed its non-adhesive core to the flow.

In the case of damage of a blood vessel wall its integrity should be restored. The blood clotting system executes this task. After a short time (several minutes), this system forms a hemostatic plug at the site of the injury, i.e., a temporary barrier which prevents blood leakage from the vessel. Disturbances in the regulation of plug formation may lead to severe disorders, from bleeding to thrombosis [6]. In order to prevent blood loss and, at the same time, to preserve the ability of blood to flow through the vessel, the hemostatic plug should have a finite size. In other words, its growth should stop when the plug has a certain size. Currently, the mechanisms

* Institut Camille Jordan, UMR 5208 CNRS, University Lyon 1, 69622 Villeurbanne, France
[2] INRIA Team Dracula, INRIA Antenne Lyon la Doua, 69603 Villeurbanne, France
[3] National Research Center for Haematology, Moscow 125167, Russia
[4] Federal Research and Clinical Centre of Paediatric Haematology, Oncology and Immunology, Moscow 117198, Russia
[5] M. V. Lomonosov Moscow State University, Moscow 119991, Russia
[6] Center for Theoretical Problems of Physicochemical Pharmacology, Moscow 119991, Russia
[7] Institute of Mechanical Engineering Problems, Saint Petersburg 199178, Russia
[8] European Institute of Systems Biology and Medicine, 69007 Lyon, France

The study was supported partly by the Russian Foundation for Basic Research grants No. 10-01-91055, 11-04-00303, 11-04-12080, 12-04-00438 and by the Russian Academy of Sciences Presidium Basic Research Programs ‘Molecular and Cellular Biology’ and ‘Basic Sciences for Medicine’, and also by the programs PICS Mathematical modelling of blood diseases (France–Russie), ANR-10-BLAN 0107 Bimod, Russian Federal programme ‘Science and Teaching for Innovation’ No. 14.740.11.0877.

that control the growth or stop the growth of a platelet plug are poorly understood despite extensive experimental and theoretical studies [3, 28].

The skeleton of a hemostatic plug is formed by aggregated platelets, i.e., specialized blood cells which are always present in blood and which are able to quickly adhere to the site of an injury and then to each other. Platelet adhesion to the active surface (a damaged vessel wall or a growing platelet aggregate) is a multi-step process: first a platelet is captured by binding its receptor GPIb to the molecules of immobilized von Willebrand factor (vWf), then the platelet becomes activated and is strongly bound to the place of the capture by its integrin receptor GPIIbIIIa [18]. The initial capture of the platelet is reversible, and most of them tear off singly or as a part of an embolus [3, 9, 18]. The space between tightly aggregated platelets is filled by fibrin polymer, which is a product of the plasma coagulation cascade [9]. Thus, the growth of a platelet plug (or a thrombus) happens through continuous removal of its exterior layers and by formation of a solid platelet-fibrin conglomerate.

The central enzyme of the plasma coagulation cascade, i.e., thrombin, which converts fibrinogen to fibrin, is also the strongest platelet activator [25]. Thrombin in a low concentration activates platelets to an adhesive state through platelet receptor PAR1 (receptors GPIIbIIIa are in the 1st affinity state); in a high concentration it activates platelets to an aggregating state through platelet receptor PAR4 (receptors GPIIbIIIa are in the 2nd affinity state) [7, 19]. However, a high concentration of thrombin and especially thrombin with collagen activate some of the platelets to a so-called coated state (receptors GPIIbIIIa are inactive, the platelet surface is densely coated with platelet-derived proteins) [8, 17, 33]. Coated platelets are not capable to aggregate, but they catalyze many reactions of the plasma coagulation cascade, i.e., the production of thrombin and fibrin. Paradoxically, a decrease in the number of these apparently procoagulant platelets is not antithrombotic, but rather accelerates thrombosis in mice [13]. The physiological role of platelet activation by these two very different routes, as well as the influence of fibrin network on platelet aggregation are unknown. However, the existence of the thrombin–coated platelets–thrombin positive feedback loop suggests that the central part of the plug (thrombus) well protected from the washing effect of the blood flow is characterized by 1) platelet activation to the coated state in the core and to aggregating state in the exterior part of the clot, and 2) a large amount of fibrin.

In this paper we propose and test in numerical simulations the following hypothesis. A platelet plug (thrombus) stops growing because of the exposure of its core to the flow. This core consists mainly of non-adhesive platelets coated and/or wrapped by a fibrin mesh; this exposure happens, as the flow removes the exterior part of the clot consisting of weakly coupled non-activated platelets.

1. Method

1.1. Dissipative particle dynamics

We use the Dissipative Particle Dynamics (DPD) method in the form described in the literature [11, 12, 16]. It is a mesoscale method, meaning that each DPD

particle describes some small volume of a simulated medium, rather than an individual molecule. The method is governed by three equations describing the conservative, dissipative, and random force acting between each two particles:

$$\mathbf{F}_{ij}^{C} = F_{ij}^{C}(r_{ij})\hat{\mathbf{r}}_{ij} \tag{1.1}$$

$$\mathbf{F}_{ij}^{D} = -\gamma\omega^{D}(r_{ij})(\mathbf{v}_{ij}\cdot\hat{\mathbf{r}}_{ij})\hat{\mathbf{r}}_{ij} \tag{1.2}$$

$$\mathbf{F}_{ij}^{R} = \sigma\omega^{R}(r_{ij})\frac{\xi_{ij}}{\sqrt{dt}}\hat{\mathbf{r}}_{ij} \tag{1.3}$$

where $\mathbf{r}_i$ is the vector of the position of the particle i, $\mathbf{r}_{ij} = \mathbf{r}_i - \mathbf{r}_j$, $r_{ij} = \left|\mathbf{r}_{ij}\right|$, $\hat{\mathbf{r}}_{ij} = \mathbf{r}_{ij}/r_{ij}$, and $\mathbf{v}_{ij} = \mathbf{v}_i - \mathbf{v}_j$ is the difference between the velocities of two particles, γ and σ are coefficients which determine the strength of the dissipative and the random force respectively, while ω^D and ω^R are weight functions; ξ_{ij} is a normally distributed random variable with zero mean, unit variance, and $\xi_{ij} = \xi_{ji}$. The conservative force is given by the equality

$$F_{ij}^{C}(r_{ij}) = \begin{cases} a_{ij}\left(1 - r_{ij}/r_c\right), & r_{ij} \leqslant r_c \\ 0, & r_{ij} > r_c \end{cases} \tag{1.4}$$

where a_{ij} is the conservative force coefficient between the particles i and j, and r_c is the cut-off radius.

The random and dissipative forces form a thermostat. If the following two relations are satisfied, the system will preserve its energy and maintain the equilibrium temperature:

$$\omega^{D}(r_{ij}) = \left[\omega^{R}(r_{ij})\right]^2, \qquad \sigma^2 = 2\gamma k_B T \tag{1.5}$$

where k_B is the Boltzmann constant and T is the temperature. The weight functions are determined by:

$$\omega^{R}(r_{ij}) = \begin{cases} \left(1 - r_{ij}/r_c\right)^k, & r_{ij} \leqslant r_c \\ 0, & r_{ij} > r_c \end{cases} \tag{1.6}$$

where $k = 1$ for the original DPD method, but it can be also varied in order to change the dynamic viscosity of the simulated fluid [11]. The motion of particles is determined by Newton's second law of motion:

$$\mathrm{d}\mathbf{r}_i = \mathbf{v}_i \mathrm{d}t, \qquad \mathrm{d}\mathbf{v}_i = \frac{\mathrm{d}t}{m_i}\sum_{j\neq i}\left(\mathbf{F}_{ij}^{C} + \mathbf{F}_{ij}^{D} + \mathbf{F}_{ij}^{R}\right) \tag{1.7}$$

where m_i is the mass of the particle i.

We have used the Euler method and a modified version of the velocity-Verlet method [1, 12], which provides better accuracy. In the former,

$$\mathbf{v}_i^{n+1} = \mathbf{v}_i^n + \frac{1}{m_i}\mathbf{F}_i\left(\mathbf{r}_i^n, \mathbf{v}_i^n\right)\mathrm{d}t \tag{1.8}$$

$$\mathbf{r}_i^{n+1} = \mathbf{r}_i^n + \mathbf{v}_i^{n+1}\mathrm{d}t \tag{1.9}$$

where indices n and $n+1$ denote time steps, and

$$\mathbf{F}_i = \sum_{j\neq i}\left(\mathbf{F}_{ij}^C + \mathbf{F}_{ij}^D + \mathbf{F}_{ij}^R\right). \tag{1.10}$$

Discretization in the second method is as follows:

$$\mathbf{r}_i^{n+1} = \mathbf{r}_i^n + \mathbf{v}_i^n\mathrm{d}t + \frac{1}{2}\mathbf{a}_i^n\mathrm{d}t^2 \tag{1.11}$$

$$\mathbf{v}_i^{n+\frac{1}{2}} = \mathbf{v}_i^n + \frac{1}{2}\mathbf{a}_i^n\mathrm{d}t, \tag{1.12}$$

$$\mathbf{a}_i^{n+1} = \frac{1}{m_i}\mathbf{F}_i\left(\mathbf{r}_i^{n+1}, \mathbf{v}_i^{n+1/2}\right) \tag{1.13}$$

$$\mathbf{v}_i^{n+1} = \mathbf{v}_i^{n+1/2} + \frac{1}{2}\mathbf{a}_i^{n+1}\mathrm{d}t \tag{1.14}$$

where a_i^n denotes the acceleration of the particle i at the nth time step. Both methods give close results.

The behaviour of the DPD method, as well as its suitability for the problem of fluid simulation is well described in the literature [10–12, 16, 23]. In [10, 11] DPD simulation results are compared with the results obtained by using continuous methods (Navier–Stokes and Stokes equations) for Couette, Poiseuille, square-cavity and triangular-cavity flow.

Simulations of the Poiseuille flow were used to calibrate the values of DPD parameters in order to make the viscosity of the simulated medium correspond to the viscosity of blood plasma [32] (≈ 1.24 mPa s). Since blood plasma can be considered as a Newtonian fluid, the viscosity of the simulated medium was calculated using the steady-state solution of 2D Navier-Stokes equations for an incompressible fluid. All simulations were done for 50μm-wide channel, density of 10^3 kg/m^3 and the average flow velocity of 2.4 cm/s. Figure 1 shows the results of the Poiseuille flow simulated with the DPD method and with the values of parameters indicated above. The density distribution is uniform and the distribution of velocity in the direction tangential to the vessel wall is parabolic. Velocity and density profiles were obtained by averaging particle density and velocity through 10^5 time steps.

1.2. Platelets

We model platelets as soft spherical particles similar to the particles of fluid in the DPD. The radius of all particles (fluid and platelets) and their mass are chosen to

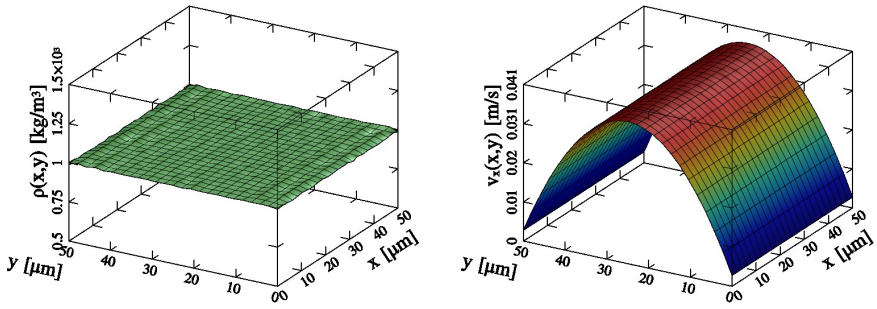

Figure 1. Poiseuille flow simulated with DPD: uniform density distribution (left) and parabolic velocity distribution (right).

correspond to the radius and the mass of the platelets. In our simulation the physical radius is set to 1μm and the mass is chosen in such a way, that the particle density corresponds to the density of the blood plasma ($\approx 10^3$ kg/m^3). The interactions between all particles are then governed by DPD, as described in the previous section, with additional adhesion force acting between the platelets. By virtue of the clot mechanical properties [5, 31], the adhesion force is modelled as a pairwise force between two platelets expressed in the form of Hooke's law:

$$\mathbf{F}^A_{ij} = k^A \left(1 - \frac{r_{ij}}{d_C}\right) \hat{\mathbf{r}}_{ij} \tag{1.15}$$

where k^A is the force strength constant and d_C is the force relaxation distance, which is equal to two times the physical radius of the platelets. As the platelet becomes bound due to its surface adhesion receptors, two platelets in the flow merge when they come in a physical contact, i.e. $r_{ij} \leqslant d_C$ (connection criterium). The platelets remain connected until their distance exceeds some critical value d_D (disconnection criterium) which is greater then d_C. We set d_D equal to 1.5 times the platelet diameter. Note that the disconnection distance can be expressed through the adhesion force.

1.3. Time-dependent platelet adhesion force

Platelet adhesion is a complex multi-step process, which involves adhesion receptors of at least two different types and the process of platelet activation [18, 26, 27]. First, the platelet is captured from the flow through weak GPIba bonding, then it is activated and forms stable adhesion through firm integrin bonding. The latter step cannot take place without the first one due to kinetic restrictions, and the first step is reversible and cannot result in stable adhesion. Since we do not explicitly introduce the kinetics of receptor binding in the model, we need to take into account the time

evolution of the adhesion force. Adhesion becomes stronger with time. A constant coefficient k^A in equation (1.15) is substituted with a time-dependent function f^A:

$$\mathbf{F}_{ij}^A = f^A(t_{ij}) \left(1 - \frac{r_{ij}}{d_C}\right) \hat{\mathbf{r}}_{ij} \tag{1.16}$$

where f^A is the function depending on time and t_{ij} is the duration of the connection between the platelets i and j. We study two cases: the first, in which the function f^A is linear, and the second, in which f^A is a step function.

In the linear case the function f^A is defined in the following way:

$$f^A(t_{ij}) = a_A t_{ij} + b_A \tag{1.17}$$

where b_A is the initial adhesion force strength, and a_A is the increase rate of the adhesion force. In the step function case, f^A is defined as follows:

$$f^A(t_{ij}) = \begin{cases} f_w^A, & t_{ij} < t_c \\ f_s^A, & \text{otherwise} \end{cases} \tag{1.18}$$

where f_w^A is the strength coefficient of the weaker connection, f_s^A is the strength coefficient of the stronger connection and t_c is the time needed for the weak connection to transform into the stronger one.

1.4. Boundary conditions

As with other particle methods, an important and delicate question is how to define the boundary conditions. To simulate a part of a blood vessel in our 2D model, three types of boundaries are used: solid, inflow and outflow. Depending on the choice of the solid boundary conditions, density oscillations or errors in the velocity profile may occur [10, 21, 29]. Figure 1 shows the correct density and velocity profiles for the Poiseuille flow obtained with the use of the solid boundary conditions described below.

The no-slip solid boundary model, which represents a blood vessel wall, consists of two parts. The first part acts in the direction tangential to the boundary and implies the parabolic velocity profile on the particles near the walls. Tangential velocity profile is measured during the simulation and for each particle near the wall an additional force is applied in the tangential direction. A precise expression of that force is given by the equation:

$$F = m\frac{(v' - v)}{\Delta t} \tag{1.19}$$

where v is the tangential part of the current velocity of the particle, v' is the velocity given by the corresponding solution of Navier–Stokes equations for incompressible fluid in a Poiseuille flow, Δt is the time step. This ensures a correct velocity profile

in the near-wall regions of the simulation domain. Even though this model works well, a more correct model should be used in simulations with platelets.

The other part of the solid boundary model applies additional force in the normal direction to the particles near the boundary. This force replaces the force which would be acting on a particle near the boundary if there were also particles on the outer side of the boundary. In that way, the balance of DPD forces is preserved in the near-wall regions, and thus the density distribution remains the same as in the middle of the simulation domain. In order to know exactly the amount of force to apply to a particle near the solid boundary, the 'force density on a particle' in the direction perpendicular to the solid boundary is measured in the bulk of the flow [11]. Consider the particle p_i in the bulk of the flow, and assume that there are n particles within the r_c radius of the particle p_i. Let us denote those particles as $p_1, \ldots, p_n$, and parts of their coordinates which are orthogonal to the solid boundaries as $y_1, \ldots, y_n$, and similarly denote with y_i the orthogonal part of coordinates of the particle p_i. Now we can write the force density function for the particle p_i:

$$F_{p_i}(h) = \frac{1}{2} \sum_{\substack{j=1,\ldots,n \\ |y_i - y_j| \geqslant h}} \left(\mathbf{F}_{ij}^C + \mathbf{F}_{ij}^D + \mathbf{F}_{ij}^R \right) \cdot \hat{\mathbf{y}} \tag{1.20}$$

where $\hat{\mathbf{y}}$ is the unit vector orthogonal to the solid boundary.

To have a more precise force density function, we can take the average of F_{p_i} for all particles which are not in the wall region. We can also measure force density over some simulation time and again take the average.

The outflow boundary is modelled in such way that all particles crossing it are being deleted. To ensure a good density distribution near the outflow boundary, the same force density function, as the one for the solid boundary is used. This force is applied in the direction orthogonal to the outflow boundary.

The inflow boundary is, however, modelled in a more complex way. At the inflow boundary the creation of new particles which will enter our simulation domain is needed. In order to do it correctly and to create plasma and platelet particles with no predefined position, a particle generation area is used in front of our simulation domain. The generation area (GA) works independently of the simulation area (SA). The solid boundaries in the GA are modelled in the same way as in the SA, but the inflow and outflow boundaries are in fact modelled as periodic boundaries, meaning that the particle that exits GA via the outflow boundary reappears on the GA inflow boundary, creating an infinite flow loop. Besides, particles from GA do not perceive the particles from SA, but the particles from SA perceive the particles from GA. For each particle which crosses the GA outflow boundary an exact copy is made at the SA inflow boundary, and that new particle is joined the SA. Once the particle has joined the SA, it can return for a short time to GA, but it remains assigned to SA and does not influence the particles from the GA. Furthermore, when it crosses back from GA to SA, it does not generate a new particle. All this insures the integrity and correctness of the GA and non-biased creation of particles for the SA.

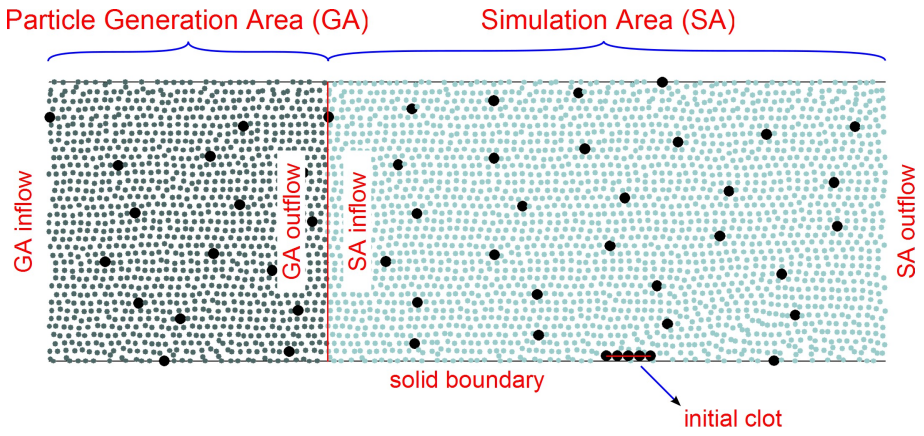

Figure 2. Particle Generation Area (GA) and Simulation Area (SA).

2. Results

The values of the parameters are chosen in such a way that they correspond to the vessel of $50\mu m$ in diameter and $150\mu m$ long (of which, the first $50\mu m$ is a Particle Generation Area followed by $100\mu m$ of Simulation Area, as shown in Fig. 2). The density and the viscosity of the simulated medium are chosen to correspond to the density and viscosity of blood plasma. The average velocity of the flow is chosen to be 24 mm/s. To initiate clotting, at the beginning of the simulation, several stationary platelets are positioned next to the lower vessel wall in the Simulation Area.

In order to verify the DPD parameters and the method applicability for non-symmetric flows, density and velocity analysis was performed in all simulations. The analysis was done by averaging the data over a short period of time. As it is shown in Fig. 1, in the simulation without a clot, the density profile was uniform and the velocity profile was parabolic. With the clot growth, the velocity profile would change with the increase of the velocity in the clot region due to narrowing of the vessel (see Fig. 3).

2.1. Constant coefficient of adhesion force strength

We study the clot growth and its dependence on the platelet adhesion force, as well as on the flow velocity, which can influence the clot growth and breakage. The latter may occur due to the flow pressure on the clot.

In the case of a constant coefficient of adhesion force (1.15) three basic types of clot growth were observed. For too small values of k^A platelets would not attach to the initial clot, while for too big values the clot would constantly grow without breaking. The most interesting behaviour was observed with medium values: the clot would grow to a certain size, and when the stress on the clot from the flow

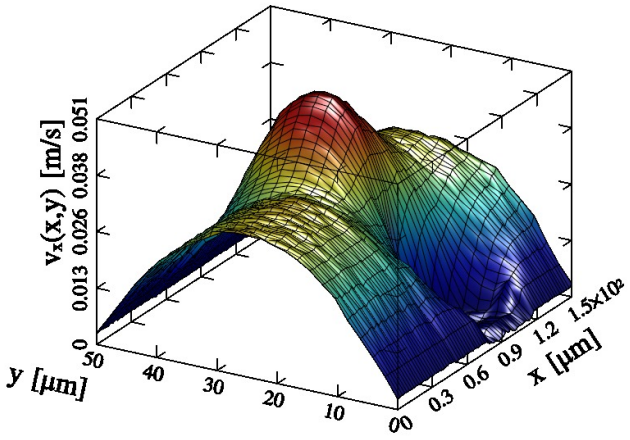

Figure 3. Velocity distribution in simulation of a flow in a blood vessel with a large clot: velocity near the clot increases due to narrowing in the blood vessel.

would overcome the strength of the adhesion forces between the platelets, the clot would break and would be carried by the flow. The snapshots of this process and its stages are shown in Fig. 4, while the clot growth in this case can be seen in Fig. 7. In simulations with a constant adhesion force the clot breaking mostly occurred near the initial clot.

2.2. Time-dependent platelet adhesion force

The use of time-dependent platelet adhesion force allowed the creation of the clot core, in which the forces between the platelets are stronger than the ones between the newly attached platelets in the outer part of the clot. In the first case, the ageing force was linear (see (1.17)). The most important stages of this simulation are presented in Fig. 5. Starting from several platelets initially placed near the boundary, the clot starts to grow. As the clot grows, the bonds between the platelets become stronger depending on the time of their attachment to the clot. When the clot becomes big enough, and the stress on it from the flow becomes too high, the part with weaker connections breaks off, leaving the core of the clot still connected to the blood vessel wall. However, as it can be seen in Fig 5, the shape of the remaining part of the clot does not correspond exactly to biological observations.

In the second case, the force ageing was introduced by a step function (1.18), which can be easier justified from the biological point of view: the transformation from weak reversible connections between platelets to strong irreversible ones happens quite quickly compared to the total time needed to complete the coagulation process. The key moments of the simulation performed with a step function model can be seen in Fig. 6. The clot grows and at the same time the core of the clot is formed. After the exterior part of the clot is removed by flow, the clot core stays attached to the blood vessel wall.

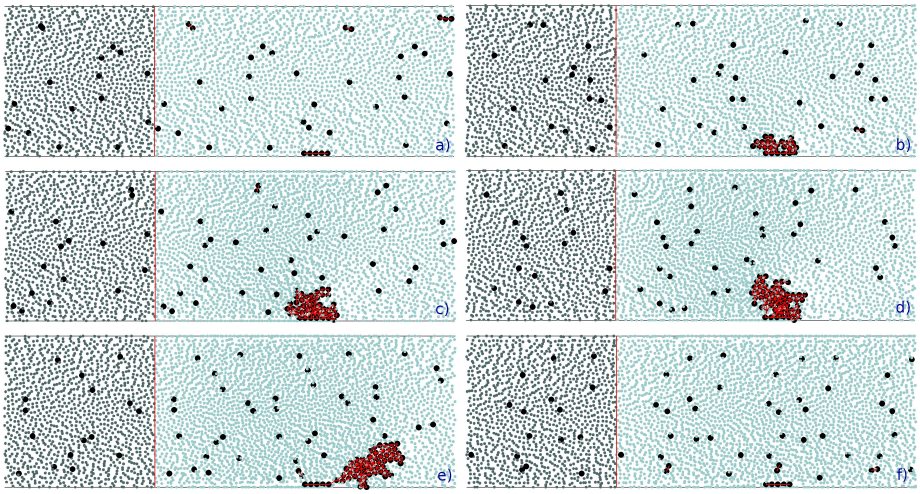

Figure 4. Snapshots of clot growth in a simulation with a constant platelet adhesion force coefficient. When it becomes sufficiently large, the force exerted by the fluid breaks the clot and it flows away.

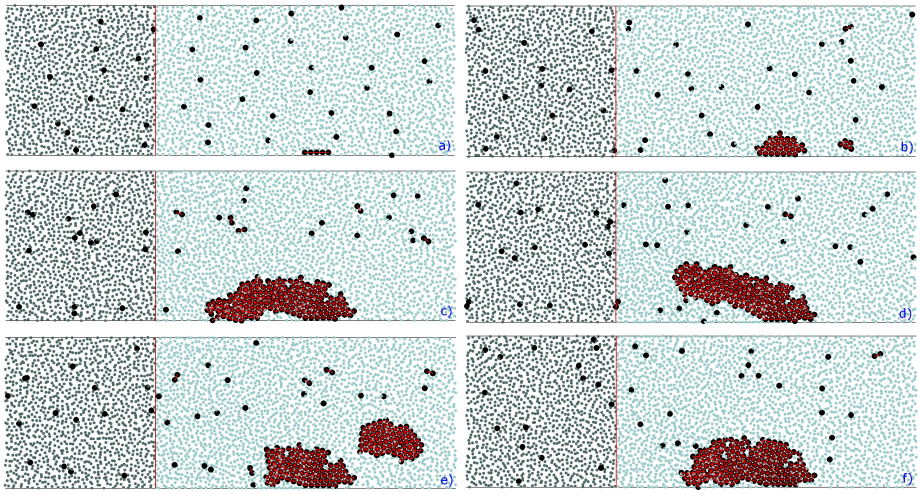

Figure 5. Snapshots of clot growth for linear time-dependent adhesion force (older connections are depicted with darker red colour): (a) initial clot, (b) small group of platelets connected with still weak adhesion forces, (c), (d) and (e) clot rupture, (f) continuation of clot growth.

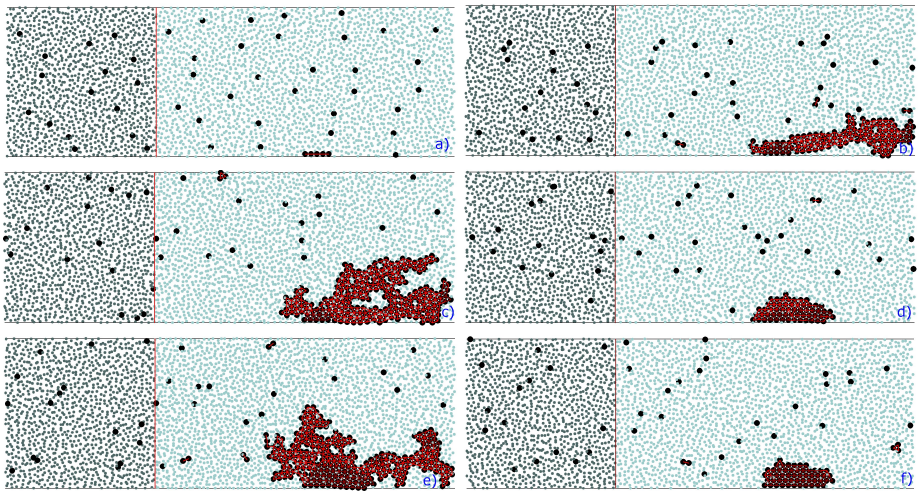

Figure 6. Snapshots of clot growth for step time-dependant adhesion force (older connections are depicted with darker red colour): (a) initial clot, (b) and (c) elongated clot with mainly weak connections, (d) clot core with mainly strong connections after rupture, (e) continued clot growth, (f) fully formed clot core after rupture.

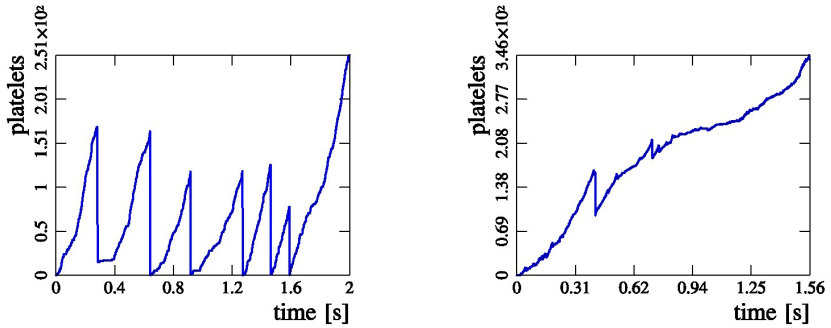

(a) (b)

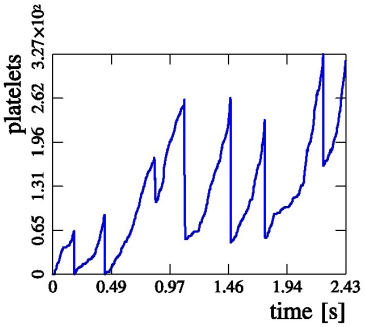

(c)

Figure 7. Clot growth and breakage for three different platelet adhesion force models : (a) constant force coefficient, (b) force coefficient as a linear function, (c) force coefficient as a step function.

Three graphs presented in Fig. 7 show the clot growth in time for the three models studied above. The first graph corresponds to the model with the constant adhesion force coefficient. It shows how with each clot rupture, the whole clot is carried away by the flow, leaving behind only the initial clot. The second graph in Fig. 7 shows how the linear model after the rupture leaves the clot core attached to the blood vessel wall. However, it also shows that the clot has a tendency to continue to grow after a rupture occurs. Finally on the last graph we can see the cloth growth for the step-function model. It shows how after some time the clot core forms, and after several subsequent ruptures, the core remains the same.

2.3. Arrest of clot growth

At the next step of this modelling, we take into account that, once a platelet becomes a part of the clot core, it is protected from connections to new platelets by a fibrin network.

In this case, we need to introduce an additional repulsing force between the platelets of the core and the new platelets coming from the flow. Indeed, now there exists the possibility of two platelets being in physical contact without becoming attached. To prevent such pairs of platelets from occupying the same space, an additional force is introduced between them. This force exists only if two non-connected platelets are in physical contact, i.e., the distance between their centres is less then the platelet diameter.

Figure 8 shows the clot growth for this modified step-function model. At the first stage of the clot growth, its mass increases linearly in time. Then the clot ruptures and does not change any more, because new platelets cannot connect to the platelets of the clot (Fig. 8a). The final form of the clot is shown in Fig. 8b. The final form of the clot for other values of parameters just after its rupture is shown in Fig.8c.

3. Discussion

One of the most important and vital issues in the field of hemostasis and thrombosis is the issue of stopping a thrombus growth. Various mechanisms have been suggested to act under different conditions, including thrombomodulin-dependent pathway [20], action of the flow [2], or fibrin ‘cup’ formation [15]. However, all these mechanisms require fibrin formation, and it is known to be strongly inhibited by the flow [24]. Here we show that this effect can be achieved via a simple regulatory mechanism, wherein the thrombus is composed of a stable core and dynamically changing loose periphery. The core is protected from the flow and is stabilized; it does not attach other platelets strongly either because of fibrin coating, or high percentage of platelets with inactivated integrins [8, 13]. Once the periphery is detached by the flow, the thrombus stops growing. Additional experiments are required to test this prediction.

In the step-function (time-dependent) model we have used time delay needed for connected platelets to become activated and strongly connected. Physiologically,

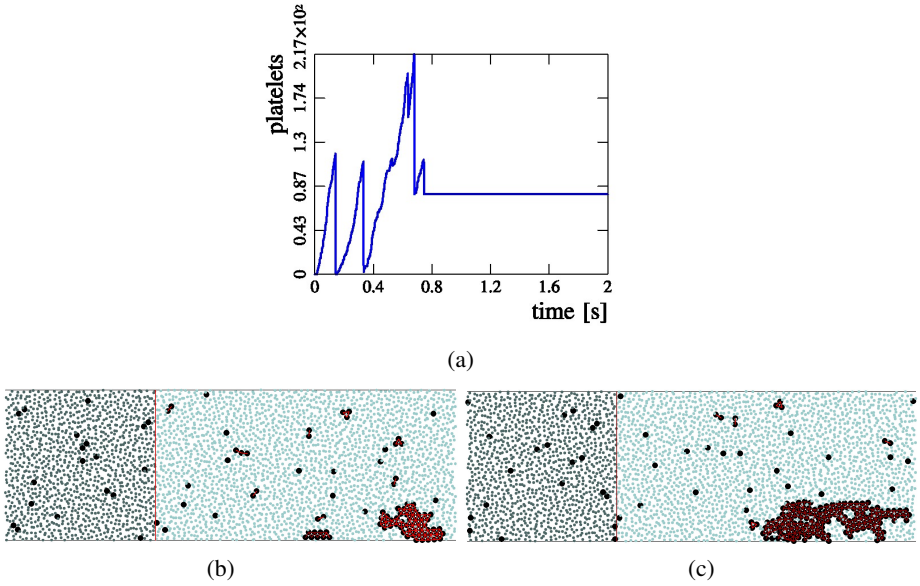

(a)

(b) (c)

Figure 8. Clot growth and breakage for the step-function model with added resistance of the clot core to adhesion of new platelets. Clot mass as a function of time (a) and final form of the clot for two sets of parameters (b) and (c).

the activation of platelets is, first of all, related to the production of fibrin and its diffusion in the flow. We do not explicitly introduce fibrin in the model and replace its effect by the time delay to reinforce the platelet connections. Therefore, this model is an approximation of a more complex phenomenon. Nevertheless, it gives an insight into modelling platelet interactions, clot growth and clot rupture. It is the first step towards a more complete model of blood coagulation where fibrin concentration would be taken into account.

Other approaches to blood coagulation modelling using particle methods are discussed in [22,30]. The forces acting on the platelets are introduced in these works in a different way. In particular, platelets are attracted to the site of the vessel wall injury, and clot growth termination is not studied.

4. Appendix. Numerical implementation

In order to develop a simulator for the described model, C++ programming language was used, because it has all the needed features. It is an intermediate-level language, which enables rapid and more robust software development and, at the same time, gives a possibility of 'low-level' optimization; it is object-oriented which enables software modularity; it is fast compared to other programming languages with similar abilities; it has a large number of already developed additional libraries, which leaves more time to focus on the model implementation. The integrated development environment (IDE) of choice was MS Visual Studio 2008, accompanied with

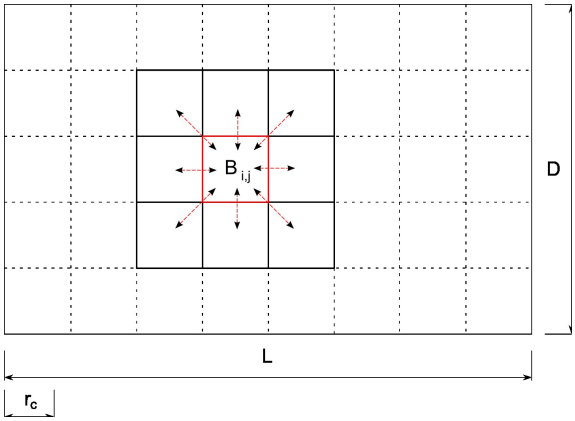

Figure 9. Schematics of optimization technique for calculation of inter-particle forces.

Microsoft Foundation Classes (MFC) for the development of the graphical user interface, OpenMP for parallelization, and MathGL for the plotting of graphs for the purpose of analysis of data generated by the simulator. All the code debugging was done in MS Visual Studio.

In DPD simulations most of the total computational time is spent on calculations of inter-particle forces, therefore, this is the part of the code where optimisation would have the largest impact. Usually, the cut-off radius of inter-particle force in DPD (r_c) is much smaller than the sizes of the simulation domain, thus the calculation of forces between all possible pairs of particles is very inefficient, because most of such pairs have an inter-particle distance larger than the cut-off radius. In order to avoid as many pairs of particles as possible, the simulation domain, a rectangle in our 2D case, can be divided into smaller rectangles (called boxes) [4] with lengths of the sides equal to $\min\{x \varepsilon \mathbf{R}^+ | x \geqslant r_c \wedge \exists\, n \varepsilon \mathbf{N}$ such that $L = nx\}$ and $\min\{y \varepsilon \mathbf{R}^+ | y \geqslant r_c \wedge \exists\, n \varepsilon \mathbf{N}$ such that $D = ny\}$, where L is the length of the domain, and D is its height. The construction of such rectangular subdivision ensures that for each particle p we can find its corresponding box $B_{i,j}$ and that all particles which have non-zero inter-particle force with particle p are contained in the box $B_{i,j}$ and 8 surrounding boxes (see Fig. 9). This eliminates most pairs of particles which have a zero inter-particle force, and therefore drastically reduces the computation time. Furthermore, the described domain subdivision enables one to easily parallelize the process of calculation of inter-particle forces by dividing the set of all pairs of 'connected' boxes into multiple disjunct subsets.

Another possibility to decrease simulation time it to increase the time step. DPD, due to its definition of conservative force as a finite function, enables a certain increase in the time step compared to other particle methods like Molecular Dynamics. However, in our simulation we had to decrease the time step more than was needed just for DPD forces, because of the much stronger forces acting between the adhered platelets (1.15).

References

1. M. P. Allen and D. J. Tidesley, *Computer Simulation of Liquids*. Clarendon, Oxford, 1987.
2. Iu. A. Barynin, I. A. Starkov, and M. A. Khanin, Mathematical models in hemostasis physiology. *Izv. Akad. Nauk Ser Biol.* (1999) No. 1, 59–66 (in Russian).
3. N. Begent and G. V. Born, Growth rate in vivo of platelet thrombi, produced by iontophoresis of ADP, as a function of mean blood flow velocity. *Nature* (1970) **227**, No. 5261, 926–930.
4. K. Boryczko, D. A. Yuen, and W. Dzwinel, *Finely Dispersed Particles, Micro-, Nano-, and Atto-Engineering*. CRC Press, 2005.
5. A. E. X. Brown, R. I. Litvinov, D. E. Discher, P. K. Purohit, and J. W. Weisel, Multiscale mechanics of fibrin polymer: gel stretching with protein unfolding and loss of water. *Science* (2009) **325**, 741.
6. R. W. Colman, A. W. Clowes, S. Z. Goldhaber, V. J. Marder, and J. N. George, *Hemostasis and Thrombosis-Basic Principles and Clinical Practice*. Lippincott Williams & Wilkins, 2006.
7. L. Covic, C. Singh, H. Smith, and A. Kuliopulos, Role of the PAR4 thrombin receptor in stabilizing platelet-platelet aggregates as revealed by a patient with Hermansky-Pudlak syndrome. *Thromb. Haemost.* 2002, V. 87, 4, P. 722-727.
8. G. L. Dale, P. Friese, P. Batar, S. F. Hamilton, G. L. Reed, K. W. Jackson, K. J. Clemetson, and L. Alberio, Stimulated platelets use serotonin to enhance their retention of procoagulant proteins on the cell surface. *Nature* (2002) **415**, No. 6868, 175–179.
9. S. Falati, P. Gross, G. Merrill-Skoloff, B. C. Furie, and B. Furie, Real-time in vivo imaging of platelets, tissue factor and fibrin during arterial thrombus formation in the mouse. *Nat. Med.* (2002) **8**, No. 10, 1175–1181.
10. D. A. Fedosov, I. V. Pivkin, and G. E. Karniadakis, Velocity limit in DPD simulations of wall-bounded flows. *J. Comp. Phys.* (2008) **227**, 2540–2559.
11. D. A. Fedosov, Multiscale modelling of blood flow and soft matter. *PhD Thesis*. Brown University, 2010.
12. R. D. Groot and P. B. Warren, Dissipative particle dynamics: Bridging the Gap Between Atomistic and Mesoscopic Simulation. *J. Chem. Phys.* (1997) **107**, No. 11, 4423–4435.
13. S. M. Jobe, K. M. Wilson, L. Leo, A. Raimondi, J. D. Molkentin, S. R. Lentz, and P. J. Di, Critical role for the mitochondrial permeability transition pore and cyclophilin D in platelet activation and thrombosis. *Blood* (2008) **111**, No. 3, 1257–1265.
14. M. M. Kamocka, J. Mu, X. Liu, N. Chen, A. Zollman, B. Sturonas-Brown, K. Dunn, Z. Xu, D. Z. Chen, M. Alber, and E. D. Rosen, Two-photon intravital imaging of thrombus development. *J. Biomed. Optics* (2010) **15**, No. 1, 16–20.
15. M. M. Kamocka, J. Mu, X. Liu, N. Chen, A. Zollman, B. Sturonas-Brown, K. Dunn, Z. Xu, D. Z. Chen, M. S. Alber, and E. D. Rosen, Two-photon intravital imaging of thrombus development. *J. Biomed. Opt.* (2010) **15**, No. 1, 16–20.
16. M. Karttunen, I. Vattulainen, and A. Lukkarinen, *A Novel Methods in Soft Matter Simulations*. Springer, Berlin, 2004.
17. Y. N. Kotova, F. I. Ataullakhanov, and M. A. Panteleev, Formation of coated platelets is regulated by the dense granule secretion of adenosine 5'diphosphate acting via the P2Y12 receptor. *J. Thromb. Haemost.* (2008) **6**, No. 9, 1603–1605.
18. S. Kulkarni, S. M. Dopheide, C. L. Yap, C. Ravanat, M. Freund, P. Mangin, K. A. Heel, A. Street, I. S. Harper, F. Lanza, and S. P. Jackson, A revised model of platelet aggregation. *J. Clin. Invest.* (2000) **105**, No. 6, 783–791.

19. A. J. Leger, L. Covic, and A. Kuliopulos, Protease-activated receptors in cardiovascular diseases. *Circulation* (2006) **114**, No. 10, 1070–1077.

20. M. A. Panteleev, M. V. Ovanesov, D. A. Kireev, A. M. Shibeko, E. I. Sinauridze, N. M. Ananyeva, A. A. Butylin, E. L. Saenko, and F. I. Ataullakhanov, Spatial propagation and localization of blood coagulation are regulated by intrinsic and protein C pathways, respectively. *Biophys.* (2006) **90**, No. 5, 489–500.

21. I. V. Pivkin and G. E. Karniadakis, A new method to impose no-slip boundary conditions in dissipative particle dynamics. *J. Comp. Phys.* (2005) **207**, 114–128.

22. I. V. Pivkin, P. D. Richardson, and G. Karniadakis, Blood flow velocity effects and role of activation delay time on growth and form of platelet thrombi. *PNAS* (2006) **103**, No. 46, 17164-17169.

23. U. D. Schiller, Dissipative particle dynamics. A study of the methodological background. *Diploma Thesis*. Faculty of Physics University of Bielefeld, Bielefeld, 2005.

24. A. M. Shibeko, E. S. Lobanova, M. A. Panteleev, and F. I. Ataullakhanov, Blood flow controls coagulation onset via the positive feedback of factor VII activation by factor Xa. *BMC Syst. Biol.* (2010) **4**, No. 5.

25. R. D. Smith and W. G. Owen, Platelet responses to compound interactions with thrombin G. *Biochemistry* (1999) **38**, No. 28, 8936–8947.

26. A. A. Tokarev, A. A. Butylin, E. A. Ermakova, E. E. Shnol, G. P. Panasenko, and F. I. Ataullakhanov, Finite platelet size could be responsible for platelet margination effect. *Biophys.* (2011) **101**, No. 8, 1835–1843.

27. A. A. Tokarev, A. A. Butylin, and F. I. Ataullakhanov, Platelet transport and adhesion in shear blood flow: the role of erythrocytes. *Comp. Res. Modelling* (2012) **4**, No. 1, 185–200 (in Russian).

28. A. Tokarev, I. Sirakov, G. Panasenko, V. Volpert, E. Shnol, A. Butylin, and F. Ataullakhanov, Continuous mathematical model of platelet thrombus formation in blood flow. *Russ. J. Numer. Anal. Math. Modelling* (2012) **27**, No. 2, 191–212.

29. A. Tosenberger, V. Salnikov, N. Bessonov, E. Babushkina, and V. Volpert, Particle dynamics methods of blood flow simulations. *Math. Model. Nat. Phenom.* (2011) **6**, No. 5, 320–332.

30. K. Tsubota, S. Wada, H. Kamada, Y. Kitagawa, R. Lima, and T. Yamaguchi, A particle method for blood flow simulation, application to flowing red blood cells and platelets. *J. Earth Simul.* (2006) **5**, 2–7.

31. J. W. Weisel, Enigmas of blood clot elasticity. *Science* (2008) **320**, 456.

32. U. Windberger, A. Bartholovitsch, R. Plasenzotti, K. J. Korak, and G. Heinze, Whole blood viscosity, plasma viscosity and erythrocyte aggregation in nine mammalian species: reference values and comparison of data. *Exp. Physiol.* (2003) **88**, 431–440.

33. J. L. Wolfs, P. Comfurius, J. T. Rasmussen, J. F. Keuren, T. Lindhout, R. F. Zwaal, and E. M. Bevers, Activated scramblase and inhibited aminophospholipid translocase cause phosphatidylserine exposure in a distinct platelet fraction. *Cell Mol. Life Sci.* (2005) **62**, No. 13, 1514–1525.

34. Z. Xu, N. Chen, M. M. Kamocka, E. D. Rosen, and M. Alber, A multiscale model of thrombus development, *J. Royal Soc. Interface* (2008) **5**, No. 24, 705–722.

35. Z. Xu, J. Lioi, J. Mu, M. M. Kamocka, X. Liu, D. Z. Chen, E. D. Rosen, and M. Alber, A multiscale model of venous thrombus formation with surface-mediated control of blood coagulation cascade. *Biophys.* (2010) **98**, No. 9, 1723–1732.

36. Z. Xu, M. Kamocka, M. Alber, and E. D. Rosen, Computational approaches to studying thrombus development. *Arterioscler. Thromb. Vasc. Biol.* (2011) **31**, No. 3, 500–505.